Estimating protein-protein interaction affinity in living cells using quantitative Förster resonance energy transfer measurements

Huanmian Chen*
Henry L. Puhl III
Stephen R. Ikeda
National Institutes of Health
National Institute on Alcohol Abuse and Alcoholism
Laboratory of Molecular Physiology
Section on Transmitter Signaling
Bethesda, Maryland 20892

Abstract. We have previously demonstrated that Förster resonance energy transfer (FRET) efficiency and the relative concentration of donor and acceptor fluorophores can be determined in living cells using three-cube wide-field fluorescence microscopy. Here, we extend the methodology to estimate the effective equilibrium dissociation constant (K_d) and the intrinsic FRET efficiency (E_{max}) of an interacting donor-acceptor pair. Assuming bimolecular interaction, the predicted FRET efficiency is a function of donor concentration, acceptor concentration, K_d, and E_{max}. We estimate K_d and E_{max} by minimizing the sum of the squared error (SSE) between the predicted and measured FRET efficiency. This is accomplished by examining the topology of SSE values for a matrix of hypothetical K_d and E_{max} values. Applying an *F*-test, the 95% confidence contour of K_d and E_{max} is calculated. We test the method by expressing an inducible FRET fusion pair consisting of FKBP12-Cerulean and Frb-Venus in HeLa cells. As the K_d for FKBP12-rapamycin and Frb has been analytically determined, the relative K_d (in fluorescence units) could be calibrated with a value based on protein concentration. The described methodology should be useful for comparing protein-protein interaction affinities in living cells.
[DOI: 10.1117/1.2799171]

Keywords: Förster resonance energy transfer; protein-protein interaction; fluorescent proteins.

Paper 07065R received Feb. 27, 2007; revised manuscript received May 14, 2007; accepted for publication May 24, 2007; published online Oct. 24, 2007.

1 Introduction

Förster resonance energy transfer (FRET) is a physical process in which a donor fluorophore molecule in the excited state transfers energy nonradiatively to an acceptor molecule (often also a fluorophore) in the ground state.[1,2] FRET occurs over distances of molecular scale (1 to 10 nm) and can thus be used to evaluate protein-protein interaction in living cells. The recent development of spectrally diverse fluorescent proteins (FP) that serve as genetically encoded donor and acceptor fluorophore tags has greatly facilitated FRET measurements in living cells.[3,4]

FRET is most appropriately quantified using the FRET efficiency, an instrument-independent index defined as the proportion of donor molecules that transfer excitation state energy to acceptor molecules.[4] In living cells expressing proteins fused with FPs, FRET efficiency can be accurately determined using donor fluorescence lifetime or sensitized acceptor emission intensity.[5] However, equating FRET efficiency with protein-protein interaction presents a challenge, as FRET efficiency is a function of multiple variables. The variables include the intracellular concentrations of donor and acceptor fluorophores (usually proteins fused to FPs), the affinity (i.e., the equilibrium dissociation constant K_d) of the interacting proteins, and the intrinsic FRET efficiency (E_{max}) of the donor/acceptor pair. Moreover, FRET efficiency is not linearly related to these variables with the exception of E_{max}. Therefore, protein pairs with disparate K_d values may display indistinguishable measured FRET efficiencies, while protein pairs with identical K_d values may display different measured FRET efficiencies.[4] Hence, the measured FRET efficiency *per se* is not an appropriate estimator of the protein-protein binding affinity.

Estimation of the binding affinity is an important goal of protein-protein interaction assays. Erickson, Alseikhan, and Peterson, and Erickson et al.[6,7] were the first to demonstrate the feasibility of using quantitative "three-cube" FRET measurements[8,9] to estimate the relative K_d of two proteins tagged with genetically encoded fluorophores expressed in living cells. However, the methodology required determination of several parameters measured from purified donor and acceptor fluorescent proteins, and detailed knowledge of the

*Current address: Department of Neuroscience, School of Medicine, Johns Hopkins University, Baltimore 21205.
Address all correspondence to: Stephen R. Ikeda, Laboratory of Molecular Physiology, NIH/NIAAA, 5625 Fishers Lane, Room TS11A, MSC 9411, Bethesda, Maryland 20892-9411; Tel: 301–443–2807; Fax 301–480–0466; E-mail: sikeda@mail.nih.gov

1083-3668/2007/12(5)/054011/9/$25.00 © 2007 SPIE

optical filter characteristics (e.g., the average molar extinction coefficient of donor and acceptor fluorophores over the bandwidth of the FRET cube excitation filter).[6,7] Moreover, the equivalence of the fluorescent protein spectra determined *in vitro* and *in vivo* (i.e., a cellular context) was assumed.

Here, we describe a method to estimate the relative K_d of two FP-tagged interacting proteins, which avoids these requirements and is performed using standard fluorescence microscopy and quantitative imaging techniques. The method was validated using an inducible FRET pair consisting of the FPs Cerulean and Venus fused to FKBP12 (a rapamycin-binding protein) and the Frb domain of FRAP1/mTOR, respectively. Upon addition of rapamycin, a complex with defined structure, stoichiometry, and affinity forms.[10]

2 Methods

In plasmid constructs used in this study, transcription was driven by the human cytomegalovirus promoter and the start codon was under the optimal context for translational initiation.[11] The constructs encoding monomeric (A206K mutation) Cerulean and Venus, variants of cyan fluorescent protein (CFP) and yellow fluorescent protein (YFP); respectively, have been previously described.[12–15] The open reading frames (ORFs) encoding the rapamycin-binding protein FKBP12 (GenBank accession number U69485) and the Frb domain of FRAP1/mTOR (GenBank accession number NM_019906; residues 2018-2114) were amplified using the polymerase chain reaction from rat whole brain cDNA (Clontech, Mountain View, California), and cloned into mammalian expression vectors encoding Cerulean and Venus, respectively. The linker sequence, KLRILQSTVPRARDPPVAT, in FKBP12-Cerulean and Frb-Venus fusion constructs was identical. The W2101F mutation was introduced into the Frb domain using the QuikChange® method (Stratagene, La Jolla, California). Frb_{W2101F} was termed Frb_{KTF} in the original description of the mutation.[16]

HeLa cells (ATCC, Manassas, Virginia) suspended in minimal essential medium containing 10% bovine calf serum were plated onto glass-bottom tissue culture dishes (MatTek, Ashland, Massachusetts) and stored in a humidified atmosphere containing 5% CO_2 in air at 37 °C. HeLa cells were transfected with plasmids using Lipofectamine 2000 (Invitrogen, Carlsbad, California) for approximately 24 h. Prior to image acquisition, culture medium was replaced with phosphate buffered saline (PBS) containing 1 mM $CaCl_2$ and $MgCl_2$. To induce heterodimerization, rapamycin (Biomol, Plymouth Meeting, Pennsylvania) was added to the PBS (1 μM final concentration) at least 40 min prior to imaging.

The imaging procedure has been described.[17] Briefly, an Olympus IX-71 inverted microscope equipped with a 75-W xenon arc lamp (Cairn Research, Kent, United Kingdom), a UNIBLITZ mechanical shutter (Vincent Associates, Rochester, New York), a 60× oil immersion objective (NA 1.4), a CFP filter set (I_{DD} cube, the donor channel; excitation: 436±10 nm, emitter: 480±20 nm, dichroic: 455LP), a YFP filter set (I_{AA} cube, the acceptor channel; excitation: 500±10 nm, emitter: 540±15 nm, dichroic: 520LP), and a FRET filter set (I_{DA} cube, the FRET channel; excitation: 436±10 nm, emitter: 540±15 nm, dichroic: 455LP). Using a 12-bit cooled charge-coupled device (CCD) camera (Retiga Exi, Qimaging, Burnaby, British Columbia, Canada) and a custom IGOR Pro (version 5, WaveMetrics, Lake Oswego, Oregon) based program, three fluorescence intensity images, i.e., I_{DD}, I_{DA}, and I_{AA} images of HeLa cells coexpressing Venus (or Venus-tagged protein) and Cerulean (or Cerulean-tagged protein) were acquired using the I_{DD}, I_{DA}, and I_{AA} filter cubes. Background fluorescence measured from untransfected cells was subtracted from all images. Images were acquired at room temperature (22 to 23 °C) with exposure times of 0.1 to 1.5 s, analog gain was set to 1, and binning set to 2×2. Fluorescence intensities were normalized to an exposure duration of 1 s. Due to the overlap of the excitation and emission spectra of Cerulean and Venus, the fluorescence intensity of the I_{DD}, I_{DA}, and I_{AA} images had three potential sources: the donor fluorescence (I_{dd}), the sensitized acceptor emission (F_c) due to FRET, and the direct acceptor emission (I_{aa}). To isolate these components in each pixel of intensity images, standard procedures and formulae have been employed.[9,18,19] I_{DD}, I_{DA}, and I_{AA} images of HeLa cells expressing only Venus were acquired, and two cross talk parameters were determined: $a=I_{DA}/I_{AA}$ and $b=I_{DD}/I_{AA}$. In these experiments, $a=0.0335\pm0.0003$ (n=11) and $b=0.0004\pm0.0001$ (n=11). I_{DD}, I_{DA}, and I_{AA} images of HeLa cells expressing only Cerulean were acquired, and two cross talk parameters were determined: $d=I_{DA}/I_{DD}$ and $c=I_{AA}/I_{DD}$. In these experiments, $c=0.0013\pm0.0001$ (n=12) and $d=0.3769\pm0.0005$ (n=12). The pixel intensity of I_{DD}, I_{DA}, and I_{AA} images in cells coexpressing Venus (or Venus-tagged protein) and Cerulean (or Cerulean-tagged protein) were characterized with the following equations:

$$I_{DD} = I_{dd} + (b/a)F_c + bI_{aa}, \tag{1}$$

$$I_{DA} = dI_{dd} + F_c + aI_{aa}, \tag{2}$$

$$I_{AA} = cI_{dd} + (c/d)F_c + I_{aa}, \tag{3}$$

where I_{dd} was donor (Cerulean) fluorescence measured using the I_{DD} cube; F_c was the FRET-induced acceptor (Venus) sensitized emission measured using the I_{DA} cube, and I_{aa} was the direct acceptor (Venus) fluorescence measured using the I_{AA} cube. Equation (1) is essentially the same as described by Gordon et al.[9] and Eqs. (2) and (3) are essentially the same as described by Gordon et al.[9] and Tron et al.[19] From these equations, I_{aa}, I_{dd}, and F_c were isolated as follows:

$$I_{aa} = \frac{dI_{AA} - cI_{DA}}{d - ca}, \tag{4}$$

$$I_{dd} = \frac{aI_{DD} - bI_{DA}}{a - bd}, \tag{5}$$

$$F_c = I_{DA} - aI_{aa} - dI_{dd}. \tag{6}$$

Previously we have demonstrated that expressing two donor-acceptor fusion FPs with differing FRET efficiencies allows us to determine: 1. the ratio of sensitized acceptor emission to donor fluorescence quenching (G factor), and 2. the ratio of donor/acceptor fluorescence intensity for equimo-

lar concentrations in the absence of FRET (k factor).[17] G and k factors are constant for given donor/acceptor pairs and a particular imaging setup. Following determination of the G and k factors for the FPs Cerulean and Venus, the FRET efficiency (E) and the concentration ratio D/A of donor (Cerulean or Cerulean-tagged protein) and acceptor (Venus or Venus-tagged protein) fluorophore can be determined:[17,18]

$$E = \frac{F_c/G}{I_{dd} + F_c/G}, \tag{7}$$

$$\frac{D}{A} = \frac{I_{dd} + F_c/G}{I_{aa}k}. \tag{8}$$

Note that I_{aa} is proportional to the intracellular concentration of the acceptor, as FRET does not alter I_{aa}. Thus we can use I_{aa} to represent the relative acceptor concentration (A). Conversely, donor fluorescence intensity is altered by FRET (i.e., donor quenching). However, the quenched fluorescence can be numerically restored by addition of the term F_c/G and the relative donor concentration (D) equated to the acceptor fluorescence intensity by normalization with the k factor. Thus,

$$A = I_{aa}, \tag{9}$$

$$D = (I_{dd} + F_c/G)/k. \tag{10}$$

Using three-cube fluorescence microscopy, I_{aa}, I_{dd}, and F_c were determined on a pixel-by-pixel basis, therefore E and the D/A were also calculated on a pixel-by-pixel basis. In these experiments, the mean values of E and D/A from single cells were used for subsequent estimation of K_d. Results are reported as mean ± SEM.

3 Theory

Assuming a bimolecular interaction between donor and acceptor molecules, a formalism derived from receptor-ligand binding studies can be adopted, in which we equate the donor and acceptor molecules to receptor and ligand, respectively. In this study, the acceptor was not expressed in great excess relative to the donor, thus we did not assume that "free" acceptor concentration was approximated by total acceptor concentration (i.e., A). The situation is equivalent to binding experiments with ligand depletion:[20]

$$D_{\text{free}} + A_{\text{free}} \underset{k_{\text{off}}}{\overset{k_{\text{on}}}{\rightleftharpoons}} DA, \tag{11}$$

$$D = D_{\text{free}} + DA, \tag{12}$$

$$A = A_{\text{free}} + DA, \tag{13}$$

$$K_d = k_{\text{off}}/k_{\text{on}}, \tag{14}$$

in which D_{free}, A_{free}, and DA are the free (i.e., uncomplexed) donor, free acceptor, and donor-acceptor concentrations, respectively. D and A are the total donor and acceptor concentrations, respectively. The on and off rate constants are denoted k_{on} and k_{off}, respectively, and K_d is the equilibrium dissociation constant. At equilibrium, the concentration of the donor-acceptor complex is described by the multivariate function:[20]

$$DA = 0.5 \times \{(A + D + K_d) - [(A + D + K_d)^2 - 4A \times D]^{1/2}\}. \tag{15}$$

The predicted FRET efficiency (E_{pred}) in a two-molecule system, as described here, is:

$$E_{\text{pred}} = (DA/D) \times E_{\max}, \tag{16}$$

where DA/D is the fractional occupancy of donor with acceptor molecules, and $E_{\max}$ is the intrinsic FRET efficiency of an interacting donor-acceptor pair.[21] Thus, combining Eqs. (15) and (16), E_{pred} for any given D and A is:

$$E_{\text{pred}} = E_{\max} \times 0.5 \times \{(A + D + K_d) - [(A + D + K_d)^2 - 4A \times D]^{1/2}\}/D. \tag{17}$$

Since A and D are measured in units of acceptor fluorescence (instead of concentration units), K_d is expressed in these units as well.

We can determine D, A, and E for cells expressing varying concentrations and ratios of interacting proteins fused to Cerulean and Venus [see Eqs. (7), (9), and (10)]. Treating D and A as independent variables, and E as the dependent variable, the free parameters K_d and $E_{\max}$ are adjusted to minimize the difference between the experimental and predicted results. Based on maximum likelihood analysis, the best estimates of K_d and $E_{\max}$ result from using the sum of the squared residual error (SSE) as the figure-of-merit function:[22,23]

$$\text{SSE} = \sum (E - E_{\text{pred}})^2. \tag{18}$$

Strictly speaking, neither A nor D are true independent variables, as both are subject to experimental errors. However, as the value of c, one of the cross talk parameters [see Eqs. (3), (4), and (9)] was very small ($c = 0.0013 \pm 0.0001$), I_{aa} (i.e., A) was nearly equal to I_{AA}, thus A could be directly measured with the I_{AA} cube. Moreover, as A was determined from the mean pixel value of I_{aa}, photon counting errors were negligible. We thus treat A as an independent variable. The determination of the relative donor concentration D involves additional calculations [see Eq. (10)]. We have previously demonstrated that D/A can be measured accurately,[17] thus D was also treated as an independent variable. Another assumption was a Gaussian distribution of E residuals—a point we examine later in the manuscript.

The remaining task was to determine a method for adjusting the parameters K_d and $E_{\max}$ to find the minimum SSE ($\text{SSE}_{\min}$). Although various iterative algorithms exist for curve-fitting multivariate functions, we chose the simple, but computationally intense, approach of computing the SSE for each dataset from a large matrix of hypothetical K_d and $E_{\max}$ values. The approach is feasible, because meaningful values of K_d and $E_{\max}$ are constrained. For example, $E_{\max}$ must lie in the range 0 to 1 to be interpretable. Moreover, given the crystal structure of fluorescent proteins, we can restrict this range even more, as the beta barrel encapsulating the fluorophore

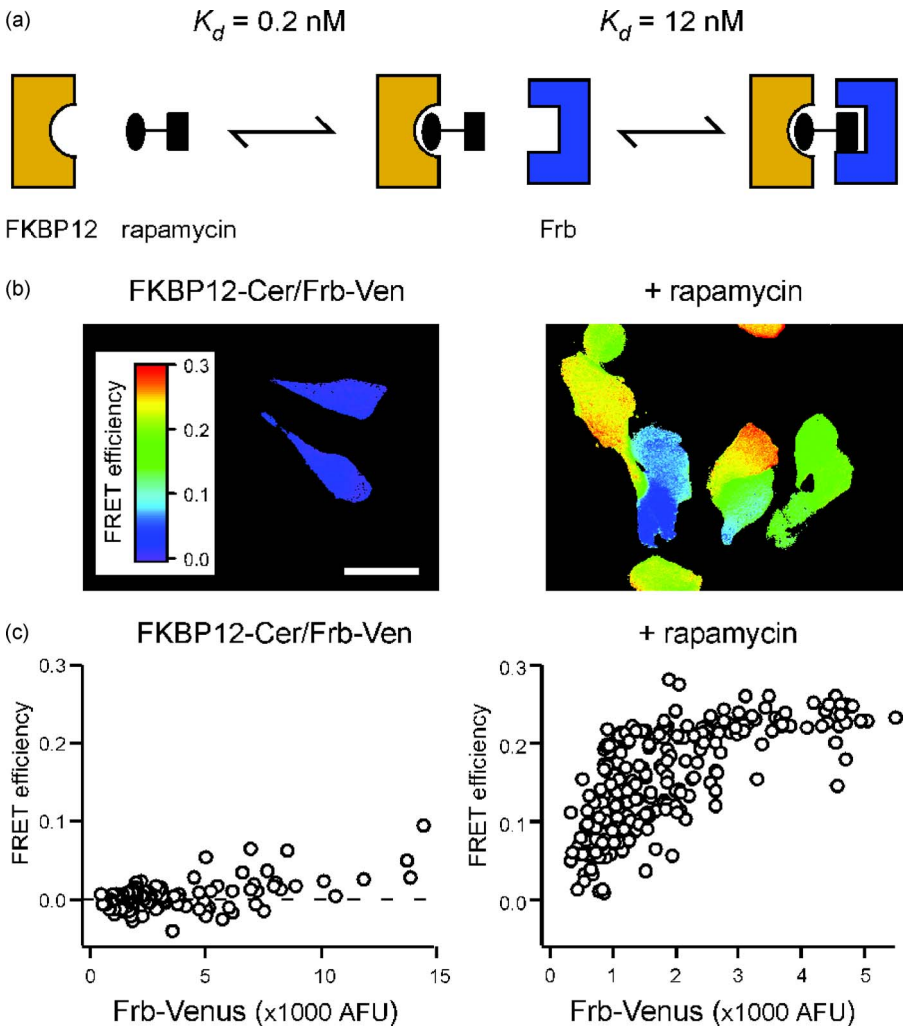

Fig. 1 Rapamycin-induced FRET. (a) Schematic diagram representing the binding events involved in the formation of FKBP12-rapamycin-Frb ternary complex. Adapted from Ref. 10. (b) Representative images illustrating FRET efficiencies (displayed using a color scale) in HeLa cells coexpressing FKBP12-Cerulean and Frb-Venus. FRET efficiencies were determined on a pixel-by-pixel basis in the absence (left panel) or presence (right panel) of 1 μM rapamycin. Scale bar, 30 μm. (c) Ensemble data illustrate FRET efficiencies measured in the absence (left) or presence (right) of 1 μM rapamycin in HeLa cells coexpressing FKBP12-Cerulean and Frb-Venus. The mean pixel FRET efficiencies from individual cells (open circles) are plotted versus the relative acceptor (Frb-Venus) concentration, in arbitrary fluorescence units (AFU). (Color online only.)

residues prevents close apposition of the donor and acceptor fluorophores. Similarly, K_d cannot be negative and the practical upper limit (that can be determined) is influenced by other factors (e.g., collisional FRET, see next). Computing the SSE_{min} in this manner provides several advantages. First, since the error for a large parameter space is computed, the method is not susceptible to finding local minimums or dependent on initial parameter values. Second, the topology of the error space provides a visual clue as to parameter correlation. Third, the method facilitates generation of a "confidence interval contour" based on a critical value of SSE determined from the F distribution.[22] Projection of this elliptical contour provides estimates of parameter confidence intervals.

4 Results

We tested our method of K_d estimation using a well-characterized inducible protein-protein heterodimerization system.[10,16,24] As shown schematically in Fig. 1(a), the protein FKBP12 has a high affinity (K_d=0.2 nM) for the cell permeable immunosuppressant, rapamycin. Subsequently, the FKBP12-rapamycin complex can bind the Frb domain of the FRAP1/mTOR protein with high affinity (K_d=12 nM), thus bringing the C-termini of FKBP12 and the Frb domains into close apposition (~15 Å). When expressed in HeLa cells, fluorescence of the fusion proteins FKBP12-Cerulean and Frb-Venus appeared distributed throughout the cytosolic and nuclear compartments (data not shown). As shown in Figs. 1(b) and 1(c) (left panels), E was negligible (0.008±0.002, n=120) in HeLa cells coexpressing FKBP12-cerulean and Frb-Venus, consistent with the idea that FKBP12 does not bind the Frb domain in the absence of rapamycin.[10] In a few cells expressing a high concentration of Frb-Venus (>5000 arbitrary fluorescence units, AFU), however, E was about 0.05. This was likely due to "collisional" FRET, as it also occurred when similar concentrations of Cerulean and Venus were expressed (data not shown). To avoid this issue, cells

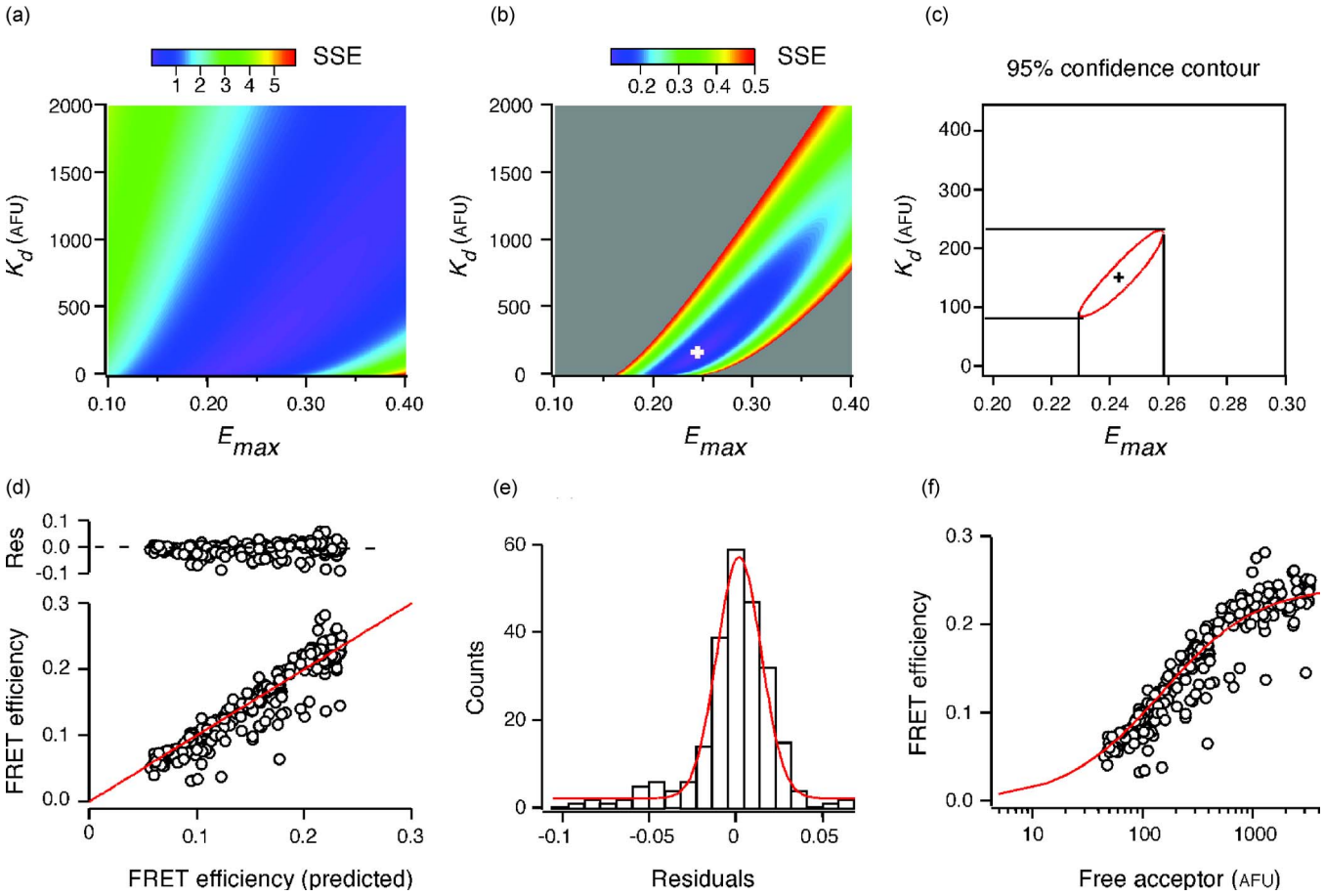

Fig. 2 Estimation of the binding affinity between rapamycin-FKBP12-Cerulean and Frb-Venus coexpressed in HeLa cells using the least square method. (a) The sum of squared errors (SSE) between the measured and predicted FRET efficiencies were generated for a matrix of K_d and E_{max} values and plotted using a color scale. (b) Same plot as in (a) using an expanded color scale. The cross indicates the minimum of the SSE. (c) The ellipse (red) defines the 95% confidence contour of the estimated K_d and E_{max}. Projections of the contour (black lines) define the estimated 95% confidence intervals of the K_d (ordinate) and E_{max} (abscissa). (d) Plot of the measured versus predicted (based on the estimated K_d and E_{max}) FRET efficiency with residuals shown before. (e) Distribution of the residuals. A Gaussian equation was fit (red line) to the histogram data. (f) The measured FRET efficiency plotted versus estimated free acceptor (Frb-Venus) concentration (in AFU). A bimolecular binding equation was fit to the data (red line). (Color online only.)

with Frb-Venus concentrations >5000 AFUs were excluded from further analysis. In addition, it has been reported that three-cube FRET measurements were prone to error when D/A fell outside the range 0.1 to 10; therefore only cells with D/A between 0.2 to 5 were chosen for further analysis.[25]

Application of rapamycin to cells coexpressing FKBP12 and Frb induces formation of the FKBP12-rapamycin-Frb complex.[10,16] Consistent with this idea, 40 min following application of a saturating concentration of rapamycin (1 μM), we detected robust FRET [$E=0.153\pm0.004$, n=248, Fig. 1(b) and 1(c), right panels] in HeLa cells coexpressing FKBP12-Cerulean and Frb-Venus. Under these conditions, all molecules of FKBP12-Cerulean should be bound to rapamycin. Thus, the trimolecular system reduces to a bimolecular system with the donor/receptor being the rapamycin-FKBP12-Cerulean complex, and the acceptor/ligand being Frb-Venus, thereby satisfying the conditions of Eqs. (15) and (17) that assume a bimolecular interaction.

To estimate the effective binding affinity (K_d) and the intrinsic FRET efficiency (E_{max}) of the rapamycin-FKBP12-Cerulean and Frb-Venus complex, HeLa cells were transfected with several different cDNA molar ratios, and an effort made to image a wide range of fluorescence intensities. E and D/A for FKBP12-Cerulean and Frb-Venus were determined using the three-filter cube approach following application of rapamycin (1 μM). In the absence of rapamycin, E varied between about −3 to 3% in cells with Frb-Venus intensity less than 5000 AFU [Fig. 1(c), left). Therefore, to increase signal-to-noise ratio, seven cells with E less than 3% in the presence of rapamycin were excluded from further analysis.

We then calculated the SSE (n=241) between the measured and predicted E using Eqs. (7), (17), and (18), custom Igor Pro-based computer program. A 448×448 array with row and column indices represented by hypothetical E_{max} (0.1 to 0.4) and K_d (0 to 2000 AFU) values, respectively, was filled with the computed SSE values for the dataset. In other words, each "pixel" in the array contained an "intensity" (i.e., z value) comprised of the SSE for the dataset computed from the corresponding K_d (ordinate) and E_{max} (abscissa). These

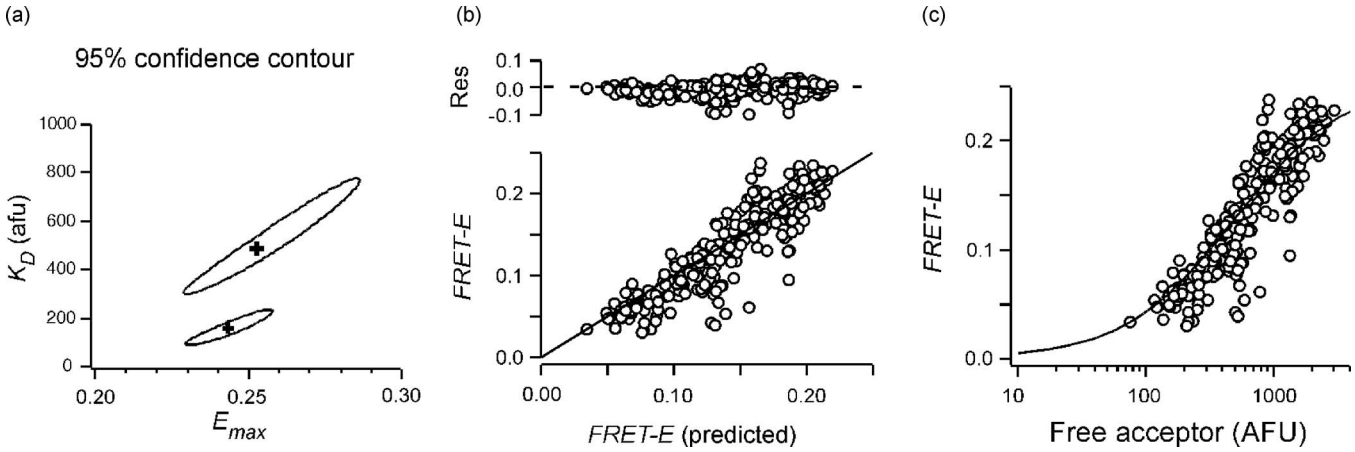

Fig. 3 Estimation of the effective binding affinity between rapamycin-FKBP12-Cerulean and the mutant Frb_{W2101F}-Venus coexpressed in HeLa cells using the least-squares method. (a) The 95% confidence contours of the estimated K_d and E_{max} for the mutant Frb_{W2101F}-Venus (upper ellipse) and wild-type Frb-Venus (lower ellipse) binding to rapamycin-FKBP12-Cerulean are displayed for visual comparison. The center of the cross indicates the point of best estimation. (b) The measured FRET efficiencies (FRET-*E*) were plotted against the corresponding predicted FRET-*E* based on the estimated K_d and E_{max}. The corresponding residuals (i.e., the difference between the measured and predicted FRET-*E*) are displayed. (c) The measured FRET-*E* are plotted versus the estimated relative concentration, in AFU, of free acceptor, Frb_{W2101F}-Venus. The data were fitted with a bimolecular binding equation.

data could be represented as an image with the SSE "intensity" coded by a color scale, as shown in Fig. 2(a) (color online only), allowing visualization of the error space topology. The band of similar colors extending diagonally across the plot indicates a "trough" in the SSE and thus parameter correlation. Expanding the color scale over a narrower range of SSE values, both the gradient [Fig. 2(b)] and convergence to the SSE_{min} (0.125, marked with a cross symbol) at K_d =148 AFU and E_{max}=0.244 become more apparent. A plot of the measured versus predicted *E*, and the corresponding residuals, is shown in Fig. 2(d). A histogram of the residuals is plotted in Fig. 2(e), and the resulting distribution fit with a Gaussian equation (solid line, p=0.12, chi-square test). This result supports an assumption of maximum likelihood analysis, on which the SSE_{min} as best estimator of K_d and E_{max} was based.[22]

To generate estimated confidence limits for K_d and E_{max}, we defined a region within the SSE space that contained all combinations of K_d and E_{max} that generated SSEs not significantly different, at an arbitrarily defined level (e.g., P=0.05), from the best-fit values. The critical value of the SSE for P =0.05 is described by:

$$SSE_{0.05} = SSE_{min}[1 + F \times p/(n-p)], \qquad (19)$$

where n is the number of data points and F is the critical value of the F distribution for a P value of 0.05, with the number of parameters (p=2) as degrees of freedom in the numerator, and n-p degrees of freedom in the denominator.[22] The critical F value can be determined in several ways, e.g., statistical tables, numerically solving the F distribution cumulative probability function, or built-in computer functions. We used the Excel (Microsoft Corporation, Redmond, Washington) function FINV(0.05,p,n-p) to determine the critical F value (version 6.0 of Igor Pro now includes the equivalent function, StatsInvFCDF). For the data illustrated in Fig. 2(a), $SSE_{0.05}$ was about 0.128, resulting in the confidence ellipse or contour (in red) illustrated in Fig. 2(c). The confidence interval for the individual parameters was calculated by projection of the confidence contour extremes onto the respective axes [Fig. 2(c), black lines]. Hence, the 95% confidence intervals of K_d and E_{max} were 83 to 230 AFU and 0.230 to 0.258, respectively. Note that the confidence intervals need not be symmetric around the best-fit values.

The data can be plotted as *E* versus free acceptor concentration (A_{free}), thereby emulating a typical saturation binding isotherm [Fig. 2(f)]. As mentioned earlier, *E* is proportional to fractional donor occupancy. A_{free} was calculated using the formula: $A_{free}=A-DA$. The data points were compared with a theoretical line generated from the previously determined E_{max} and K_d parameters according to: $E=E_{max}\times A_{free}/(K_d+A_{free})$. The data points span much of the binding curve around the K_d value—a prerequisite for accurate parameter estimation. It should be emphasized that the K_d value cannot be derived from *E* versus A_{free} relationship, as this represents a circular dependency. The main purpose of Fig. 2(f) is to provide a visual data representation analogous to radioligand binding studies.

The ability to distinguish different affinities was tested by introducing a point mutation, W2101F, in the Frb domain. Previous studies indicated that the affinity between the rapamcyin-FKBP12 complex and Frb_{W2101F} was reduced.[16] The experimental procedure used before was repeated using Frb_{W2101F}-Venus in place of the wild-type construct. As shown in Fig. 3(a) (upper ellipse), the effective K_d and E_{max} were estimated to be 492 AFU (95% confidence interval 292 to 775 AFU) and 0.255 (95% confidence interval 0.229 to 0.287), respectively. As before, we plotted the *E* measured from HeLa cells (n=261) coexpressing FKBP12-Cerulean and Frb_{W2101F}-Venus (in the presence of 1 μM rapamycin) against the E_{pred} [Fig. 3(b)]. The residuals were also calculated [Fig. 3(b)] and the distribution found to be adequately described by a Gaussian equation (data not shown). Express-

ing the data as a standard binding isotherm [i.e., E versus free acceptor concentration, Fig. 3(c)] revealed a right-shifted sigmoid curve with data points spanning the estimated K_d value. Based on these data, we conclude that the affinity between rapamycin-FKBP12-Cerulean complex and Frb_{W2101F}-Venus was significantly lower when compared with wild-type Frb-Venus. This conclusion is visually evident when the 95% confidence ellipse from Fig. 2(c) is superimposed on Fig. 3(a) (lower ellipse). Our conclusion is consistent with the results from a rapamycin-induced transcriptional switch assay performed in yeast cells using Frb_{W2101F}.[16] In contrast to the K_d, the estimated E_{max} for Frb_{W2101F} was not significantly different from the wild-type Frb. Although structural changes resulting from point mutations are difficult to predict, the result is consistent with the position of the W2101F mutation within the context of the wild-type Frb crystal structure. The mutated residue lies within the Frb-rapamycin binding pocket and thus, barring dramatic long-range alterations in conformation, would not be expected to alter the position of the Frb C-terminus where the fluorescent protein is attached, and hence the intrinsic FRET efficiency (i.e., E_{max}).

An advantage of the FKBP12-rapamycin-Frb system, aside from being inducible, is that the absolute affinity (K_d = 12 nM) has been well characterized.[10] Assuming that the *in-vivo* and *in-vitro* binding affinities are comparable and the fluorescent protein tagging has a negligible effect on binding affinity, we can calibrate our system with the literature value for the wild-type Frb and estimate that the affinity between FKBP12-rapamycin and Frb_{W2101F} in living cells to be about 40 nM (95% confidence interval 24 to 63 nM).

5 Discussion

We have described a simple optical method for estimating the effective affinity between two protein domains in living mammalian cells. This method was extended from a previous study in which E and D/A was determined in living cells using three-cube wide-field fluorescence microscopy.[17] Assuming a simple bimolecular interaction, E is a function of donor and acceptor concentrations (total, not free) and the parameters K_d and E_{max}. We estimated K_d and E_{max} by minimizing the SSE between the predicted and the measured E. Minimization was accomplished by generating SSE values for a matrix of hypothetical K_d and E_{max} values. From the topology, a 95% confidence contour for K_d and E_{max} was generated using a critical F value. Projection of the contour allowed assignment of estimated confidence intervals to each parameter. The method was tested by expressing an inducible FRET fusion pair consisting of FKBP12-Cerulean and Frb-Venus (wild-type or mutant) in HeLa cells. We demonstrated that when coexpressed in HeLa cells and in the presence of the heterodimerization-inducer rapamycin at the saturating concentration, FKBP12-Cerulean has a higher affinity for Frb-Venus than to the mutant Frb_{W2101F}-Venus. This result was consistent with a report using a transcriptional switch assay based on the yeast two-hybrid system.[16] Therefore, the described methodology is useful for comparing protein-protein interaction affinities based on FRET determinations in living cells.

5.1 *Comparison with Other Methods*

The development of our K_d estimation method was inspired by the seminal work of Erickson, Alseikhan, and Peterson, and Erickson et al.,[6,7] who first demonstrated the feasibility of estimating protein-protein interaction affinity in living cells using three-cube FRET measurements. Although similar in principle, there are several factors that differentiate the two techniques. First, the method described here relies solely on conventional fluorescent microscopy and live cell measurements. The FRET efficiency, relative donor concentration, and relative acceptor concentration were determined using methods developed in a previous study.[17] The key requirement for calibrating the measurements (i.e., the G and k factors) was development of donor-acceptor pairs (i.e., FP fusion constructs) with widely differing E and known stoichiometries (e.g., 1:1). In contrast, Erickson, Alseikhan, and Peterson, and Erickson et al.[6,7] used spectroscopic data from purified FPs and optical filters to arrive at D and A. Thus, our method requires fewer assumptions (e.g., equivalence of *in-vitro* to *in-vivo* derived constants) and is generally more accessible. Second, the method described here is based on traditional donor-based FRET efficiency measurements, whereas FRET ratio, an acceptor-based FRET index, was used in Refs. 6 and 7. Although both indices provide similar information, FRET efficiency is instrument-independent and thus comparable among different laboratories and experimental settings. Moreover, intrinsic FRET efficiency (E_{max}) provides the basis for limited inference about the distance between fluorophores. Third, although both methods are based on cellular fluorescence intensity measurements, our data were acquired with a cooled CCD camera (data for single cells represent the mean of many pixel values), whereas Erickson, Alseikhan, and Peterson, and Erickson et al.[6,7] used a photomultiplier tube to measure total cellular fluorescence intensity, and thus assume a similar cell size. Fourth, we minimized SSE by examining a subset of error space topology, while Erickson, Alseikhan, and Peterson, and Erickson et al. used an iterative routine. Computing the error space topology allows estimation of a confidence contour helpful in interpreting the fitted parameters, and avoids finding the local (instead of global) minimum, which is a potential issue inherent to most iterative algorithms. The contour includes the parameter covariance in the evaluation of the confidence intervals, thus allowing more rigorous statistical comparison of the estimated parameters.[26] The color-coded error topology graphs [e.g., Fig. 2(a) (color online only)] provide visual indication of the correlation between K_d and E_{max}. A paradoxical consequence of parameter correlation is that nonoverlapping confidence contours can result in overlapping parameter confidence intervals. In this case, K_d and/or E_{max} significantly differ, but one cannot assign the difference to an individual parameter.

FRET efficiency can be determined using fluorescence lifetimes rather than intensities. In principle, the intrinsic FRET efficiency and fractional donor occupancy (by acceptor) are directly determined from the parameters (i.e., time constants and relative amplitudes) of a multiexponential fit to the donor fluorescence decay.[27,28] For a bimolecular reaction, the relationship between fractional donor occupancy and free acceptor concentration would be described by a Langmuir binding isotherm, thus allowing K_d determination using con-

ventional analyses. However, lifetime imaging requires very expensive equipment unavailable to most laboratories, and collecting sufficient photon counts for reliable analyses can require 10 to 15 min per cell. Moreover, FRET efficiency and fractional donor occupancy determination based on FP lifetime analysis has proven more complex than anticipated. For example, linked constructs of Cerulean and Venus exhibited multiple time constants of donor fluorescence decay when only one component was predicted.[12] The reason for this discrepancy is unclear, but the phenomenon demonstrates unexpected complexity in what superficially appears to be a simple process. Whether lifetime imaging or intensity-based methods are used to estimated K_d (based on FRET efficiency) will be dictated by the resources and expertise available, and the conditions and goals of the experiment. Under some circumstances, lifetime imaging is a more reliable method to quantify FRET efficiency when compared with intensity-based measurments.[27] Conversely, for FPs imaged in living cells, intensity- and lifetime-based methods produced comparable results.[5]

5.2 *Factors Affecting Föster Resonance Eenergy Transfer Based Affinity Measurements*

There are several factors that require consideration when using FRET to estimate affinity in living cells. First, signal-to-noise ratio is maximized when the proteins under study have both a high affinity and intrinsic FRET efficiency. Estimation of low affinity interactions is compromised by "collisional" FRET. For example, if the relative K_d between two proteins is larger than ~5000 AFU, then donor occupancy cannot span a large range without incurring nonspecific FRET. Consequently, K_d estimation based on these data will be prone to error. Based on the reported *in-vitro* determined K_d of FKBP12-rapamycin and Frb, we estimate that a K_d greater than 0.4 μM will be difficult to assess unless collisional FRET efficiency can be accounted for. Maximizing intrinsic FRET efficiency helps to minimize this problem by increasing the signal above both the inherent noise floor and any collisional FRET that might occur. In this regard, two novel variants of GFP, CyPet and yPet, have been engineered to maximize FRET signals.[29] It is unclear at this time, however, whether CyPet and yPet will be superior to Cerulean and Venus for these types of studies.

Second, we assume that the mean fluorescence intensity (corrected for background and FRET) is proportional to fluorophore concentration. Ideally, each pixel would represent a constant cellular volume. With wide-field microscopy, this is unlikely, as one observes variation in fluorescence intensity within cells, even with a high NA objective (e.g., brighter over the nucleus, which is the thickest portion of the cell). Although determinations of E and D/A are not affected by this requirement, determinations of D and A are. For cells with similar morphology (such as HeLa cells), however, the mean cellular fluorescence intensity should be proportional to cellular fluorophore concentration for small soluble proteins that distribute evenly throughout the nucleus and cytoplasm. Estimation of the K_d between two plasma membrane proteins or between a plasma membrane and a cytosolic protein, however, will likely present greater challenges, as the heterogeneity in concentrations and FRET efficiencies within subcellular compartments complicates interpretation. Techniques that limit the excitation to (multiphoton or total internal reflection fluorescence microscopy) or collection of light from (confocal microscopy) a smaller cellular volume should be superior under these circumstances.

Third, the K_d estimation based on FRET measurement assumes that negligible fractions of donor or/and acceptor molecules bind to endogenous proteins. If this assumption does not hold, the K_d value will be overestimated. However, the presence of potentially interacting endogenous proteins should not affect the assessment of the affinity change arising from a point mutation. It should be noted that K_d values reported here (in AFUs) are instrument-dependent, whereas the ranking of K_d values is not.

Fourth, we emphasize the need to image cells varying in both fluorescent protein concentration and D/A ratio. The former is usually accomplished by exploiting the normally occurring variations in protein expression, i.e., imaging the entire range of dim to bright cells. The latter, however, requires transfecting several different ratios (empirically determined) of donor/acceptor cDNA. Together, the two conditions are usually sufficient to generate a wide range of donor fractional occupancy—a requirement for accurate parameter estimation. An indicator of inadequate coverage of the donor fractional occupancy range is failure of the confidence ellipse to close at one end.[22]

Finally, the current method is predicated on the assumption of a simple bimolecular interaction. It does not account for multiple binding affinities or energy transfer to multiple acceptors. Although a model accounting for additional complexity could be generated, the expansion of free parameters (and correlation between parameters) would increase parameter uncertainty and correlation—possibly beyond the point where meaningful parameter estimates are generated.

5.3 *Utility*

The use of FRET-based methods to indicate protein-protein interaction is becoming increasingly popular. However, FRET indices are primarily an indicator of proximity (if one ignores orientation factors), and any conclusions regarding protein-protein interaction require an interpretation within this context. Thus, the ability to estimate the affinity between two proteins in living cells using FRET measurements provides an additional means to evaluate FRET experiments and make judgments as to whether biologically relevant protein-protein interaction can be reasonably assumed from the measurements.

Acknowledgment

We thank Steven S. Vogel for many helpful discussions. This work was supported by the intramural program of the NIH, National Institute on Alcohol Abuse and Alcoholism, Bethesda, Maryland 20892.

References

1. H. Wallrabe and A. Periasamy, "Imaging protein molecules with FRET and FLIM microscopy," *Curr. Opin. Biotechnol.* **16**, 19–27 (2005).
2. E. A. Jares-Erijman and T. M. Jovin, "Imaging molecular interactions in living cells by FRET microscopy," *Curr. Opin. Chem. Biol.* **10**, 409–416 (2006).

3. N. C. Shaner, P. A. Steinbach, and R. Y. Tsien, "A guide to choosing fluorescent proteins," *Nat. Methods* **2**, 905–909 (2005).
4. S. S. Vogel, C. Thaler, and S. V. Koushik, "Fanciful FRET," *Sci. STKE.* **2006**(31) :re2 (2006).
5. S. V. Koushik, H. Chen, C. Thaler, H. L. Puhl 3rd, and S. S. Vogel, "Cerulean, Venus, and $Venus_{Y67C}$ FRET reference standards," *Biophys. J.* **91**, L99–L101 (2006).
6. M. G. Erickson, B. A. Alseikhan, B. Z. Peterson, and D. T. Yue, "Preassociation of calmodulin with voltage-gated Ca^{2+} channels revealed by FRET in single living cells," *Neuron* **31**, 973–985 (2001).
7. M. G. Erickson, H. Liang, M. X. Mori, and D. T. Yue, "FRET two-hybrid mapping reveals function and location of L-type Ca^{2+} channel CaM preassociation," *Neuron* **39**, 97–107 (2003).
8. R. D. Mitra, C. M. Silva, and D. C. Youvan, "Fluorescence resonance energy transfer between blue-emitting and red-shifted excitation derivatives of the green fluorescent protein," *Gene* **173**, 13–17 (1996).
9. G. W. Gordon, G. Berry, X. H. Liang, B. Levine, and B. Herman, "Quantitative fluorescence resonance energy transfer measurements using fluorescence microscopy," *Biophys. J.* **74**, 2702–2713 (1998).
10. L. A. Banaszynski, C. W. Liu, and T. J. Wandless, "Characterization of the FKBP·rapamycin·FRB ternary complex," *J. Am. Chem. Soc.* **127**, 4715–4721 (2005).
11. M. Kozak, "Initiation of translation in prokaryotes and eukaryotes," *Gene* **34**, 187–208 (1999).
12. C. Thaler, S. V. Koushik, P. S. Blank, and S. S. Vogel, "Quantitative multiphoton spectral imaging and its use for measuring resonance energy transfer," *Biophys. J.* **89**, 2736–2749 (2005).
13. T. Nagai, K. Ibata, E. S. Park, M. Kubota, K. Mikoshiba, and A. Miyawaki, "A variant of yellow fluorescent protein with fast and efficient maturation for cell-biological applications," *Nat. Biotechnol.* **20**, 87–90 (2002).
14. M. A. Rizzo, G. H. Springer, B. Granada, and D. W. Piston, "An improved cyan fluorescent protein variant useful for FRET," *Nat. Biotechnol.* **22**, 445–449 (2004).
15. D. A. Zacharias, J. D. Violin, A. C. Newton, and R. Y. Tsien, "Partitioning of lipid-modified monomeric GFPs into membrane microdomains of live cells," *Science* **296**, 913–916 (2002).
16. J. H. Bayle, J. S. Grimley, K. Stankunas, J. E. Gestwicki, T. J. Wandless, and G. R. Crabtree, "Rapamycin analogs with differential binding specificity permit orthogonal control of protein activity," *Chem. Biol.* **13**, 99–107 (2006).
17. H. Chen, H. L. Puhl III, S. V. Koushik, S. S. Vogel, and S. R. Ikeda, "Measurement of FRET efficiency and ratio of donor to acceptor concentration in living cells," *Biophys. J.* **91**, L39–L41 (2006).
18. T. Zal and N. R. Gascoigne, "Photobleaching-corrected FRET efficiency imaging of live cells," *Biophys. J.* **86**, 3923–3939 (2004).
19. L. Tron, J. Szollosi, S. Damjanovich, S. H. Helliwell, D. J. Arndt-Jovin, and T. M. Jovin, "Flow cytometric measurement of fluorescence resonance energy transfer on cell surfaces. Quantitative evaluation of the transfer efficiency on a cell-by-cell basis," *Biophys. J.* **45**, 939–946 (1984).
20. I. H. Segel, *Enzyme kinetics: Behavior and Analysis of Rapid Equilibrium and Steady-State Enzyme Systems*, Wiley-Interscience, New York (1975).
21. A. Hoppe, K. Christensen, and J. A. Swanson, "Fluorescence resonance energy transfer-based stoichiometry in living cells," *Biophys. J.* **83**, 3652–3664 (2002).
22. H. Motulsky and A. Christopoulos, *Fitting Models to Biological Data Using Linear and Nonlinear Regression. A Practical Guide to Curve Fitting*, Oxford University Press, New York (2004).
23. W. H. Press, B. P. Flannery, S. A. Teukolsky, and W. T. Vetterling, *Numerical Recipes in C: The Art of Scientific Computing*, Cambridge University Press, Cambridge, MA (1988).
24. T. Inoue, W. D. Heo, J. S. Grimley, T. J. Wandless, and T. Meyer, "An inducible translocation strategy to rapidly activate and inhibit small GTPase signaling pathways," *Nat. Methods* **2**, 415–418 (2005).
25. C. Berney and G. Danuser, "FRET or no FRET: a quantitative comparison," *Biophys. J.* **84**, 3992–4010 (2003).
26. R. Maggi and G. E. Rovati, "MacELLIPSE, a graphical aid to the problem of the joint confidence region: a practical example for ligand binding experiments," *Pharm. Res.* **28**, 351–358 (1993).
27. S. Pelet, M. J. R. Previte, and P. T. C. So, "Comparing the quantification of Förster resonance energy transfer measurement accuracies based on intensity, spectral, and lifetime imaging," *J. Biomed. Opt.* **03**, 034017 (2006).
28. R. R. Duncan, "Fluorescence lifetime imaging microscopy (FLIM) to quantify protein-protein interactions inside cells," *Biochem. Soc. Trans.* **34**, 679–682 (2006).
29. A. W. Nguyen and P. S. Daugherty, "Evolutionary optimization of fluorescent proteins for intracellular FRET," *Nat. Biotechnol.* **23**, 355–360 (2005).